SCIENCE CHINA
Information Sciences

• RESEARCH PAPER •

March 2025, Vol. 68, Iss. 3, 132301:1–132301:17
https://doi.org/10.1007/s11432-024-4265-7

Joint communication and computation design for secure integrated sensing and semantic communication system

Jianxin DAI[1,5], Hui FAN[1], Zhouxiang ZHAO[2,3], Yongjun XU[4], Zhaohui YANG[2,3*], Xu GAN[2,3] & Zhaoyang ZHANG[2,3]

[1]*School of Science, Nanjing University of Posts and Telecommunications, Nanjing 210023, China*
[2]*College of Information Science and Electronic Engineering, Zhejiang University, Hangzhou 310058, China*
[3]*Zhejiang Provincial Laboratory of Multi-Modal Communication Networks and Intelligent Information Processing, Hangzhou 310027, China*
[4]*School of Communications and Information Engineering, Chongqing University of Posts and Telecommunications, Chongqing 400065, China*
[5]*National Mobile Communications Research Laboratory, Southeast University, Nanjing 210096, China*

Received 31 July 2024/Revised 13 November 2024/Accepted 2 January 2025/Published online 11 February 2025

Abstract As a new communication paradigm, semantic communication (SC) differs from conventional communication based on bit transmission by transmitting semantic information, which demonstrates enormous potential in improving communication efficiency. To ensure transmission security, this paper investigates the secure resource allocation problem of integrated sensing and semantic communication (ISSC) systems in the scenario involving multiple eavesdroppers considering cases of both perfect and imperfect channel state information (CSI). Specifically, the concept of secure semantic rate (SSR) is first put forward to measure the reliability of user information acquisition, and then an optimization problem is formulated to maximize the secure semantic efficiency (SSE), which is defined as the ratio of the sum of SSRs to total transmit power. To work out this problem, the optimization problem is first decoupled into two subproblems, i.e., beamforming optimization subproblem and semantic parameter optimization subproblem. For the beamforming optimization subproblem, this paper simplifies the objective function by utilizing the Dinkelbach algorithm with given semantic parameters and proposes an alternating algorithm to solve a series of convex subproblems iteratively. For the semantic parameter subproblem, the monotonically decreasing property of the objective function with respect to the semantic parameter is revealed mathematically under a given beamforming vector. Finally, simulation results verify the theoretical analysis.

Keywords integrated sensing and semantic communication (ISSC), resource allocation, beamforming design, security, robust optimization

Citation Dai J X, Fan H, Zhao Z X, et al. Joint communication and computation design for secure integrated sensing and semantic communication system. Sci China Inf Sci, 2025, 68(3): 132301, https://doi.org/10.1007/s11432-024-4265-7

1 Introduction

With the increasing demand for artificial intelligence (AI) services, the sixth-generation (6G) wireless network is shifting from the previous focus on high transmission rates to a new architecture called semantic communication (SC) [1]. Unlike conventional communication which transmits complete source information, SC concentrates on extracting and transmitting semantic meanings [2]. Specifically, at the transmitter side, the core semantics are encoded, while they are decoded and reconstructed at the receiver side [3] based on shared knowledge bases such as those constructed by probabilistic graphical models [4]. Researchers have explored different types of semantic encoding and decoding systems for various types of source information. The authors in [5] addressed task-oriented communication based on different modalities, including image retrieval, machine translation, and visual question answering (VQA). SC, as one of the key technologies for 6G wireless communication, benefits from the development and application of machine learning (ML) and deep learning (DL) in its implementation [6]. Depending on the type of source data, different ML models are constructed for SC systems. For text information, methods such

* Corresponding author (email: yang_zhaohui@zju.edu.cn)

as long short term memory (LSTM) [7] and Transformer [8] are considered, based on which the authors propose the deep learning-enabled semantic communication (DeepSC) model. For image data, deep neural network (DNN) [9] can be considered, and for speech data, convolutional neural network (CNN) [10] is a potential option. The SC studied in this paper focuses on the transmission of text, and therefore, DeepSC is adopted to model the SC system presented herein. SC integrates communication and computation by sacrificing some redundant data to compress the source data, thereby significantly improving communication efficiency [11]. Although SC greatly reduces communication consumption through computation, the resulting computation consumption cannot be ignored. Therefore, it is necessary to conduct resource allocation research on joint communication and computation design for SC [12]. Researchers have conducted resource allocation of SC systems in vehicle networking [13] and simultaneous wireless information and power transfer (SWIPT) scenarios [14], and accordingly proposed the optimal resource allocation schemes.

However, due to the inherent broadcast characteristic of wireless channels [15], along with the susceptibility of deep neural networks [16], SC systems become more susceptible to malicious eavesdropping. Therefore, in order to ensure communication reliability, it is necessary to research the security issues of communication [17]. Previous research has extensively studied the security of conventional wireless communication. The authors in [18] explored the covert communication within a non-orthogonal multiple access (NOMA) system which is assisted by an intelligent reflecting surface (IRS). In [19], the authors considered the problem of secure resource allocation in the presence of base stations (BSs), users, eavesdroppers, and energy harvesters. The work in [20] proposed a robust artificial noise-assisted secure transmission scheme for SWIPT in multiple-input multiple-output (MIMO) communication systems with multiple eavesdroppers. Although some researchers have studied the security of SC systems, such as the DL driven joint source-channel coding (DeepJSCC) scheme proposed in [21] for wireless image transmission, which provided security against eavesdropper attacks. To the best of our knowledge, there are very few existing studies on secure SC that involve resource allocation. In [22], the authors consider a secure resource allocation scheme in an integrated sensing and semantic communication (ISSC) system, aiming to maximize the secure semantic rate (SSR) while ensuring sensing performance. Currently, there is no research on the secure semantic efficiency (SSE) of ISSC systems. The research on SSE in this paper fills this gap. Previous research on resource allocation and security for communication systems generally assumed that perfect channel state information (CSI) is available. However, in reality, due to the randomness of channels and potential errors or quantization effects that may occur during CSI estimation [23], it is extremely difficult to obtain perfect CSI. Meanwhile, successful security configurations for communication systems require the assumption of a worst-case scenario, where the hardware resources and computation capabilities held by eavesdroppers far exceed those owned by legitimate users [24]. Additionally, eavesdroppers are not continuously interacting with BSs, which poses a significant challenge for BSs to obtain perfect CSI regarding eavesdroppers. Therefore, when designing secure resource allocation schemes, the uncertainty of eavesdroppers' CSI needs to be taken into account. There are mainly two types of uncertainty models for CSI: deterministic models and stochastic models [25]. Deterministic models employ deterministic, bounded additive uncertainty sets, assuming that CSI errors are bounded variables. On the other hand, stochastic models assume that CSI errors are random variables that follow specific distributions [26].

Integrated sensing and communication (ISAC) has become a focal point of contemporary research due to its ability to merge communication and sensing capabilities into a single system, thereby optimizing resource utilization and enhancing overall system performance [27, 28]. ISAC can facilitate a myriad of applications, including autonomous vehicles [29], smart cities [30], and advanced manufacturing, by providing high-resolution sensing and robust communication simultaneously. However, research on sensing tasks within SC remains a promising field that has been insufficiently explored. Sending semantically processed and compressed signals not only enhances system energy efficiency under conditions of limited communication resources but also improves signal utilization by reusing SC signals for target sensing. Furthermore, in response to the requirements of next-generation internet applications for low latency, high reliability, and immersive experiences, integrating SC-one of the key technologies of 6G wireless communication-with sensing not only facilitates more convenient and efficient access to wireless networks for users but also enables more precise and effective target location and activity monitoring. Pushing AI to the edge of the network has become a consensus, giving rise to the research field of edge intelligence, which seamlessly integrates sensing, communication, and computation in a task-oriented manner to address the demands of emerging applications [31]. Specifically, it aids in constructing virtual worlds

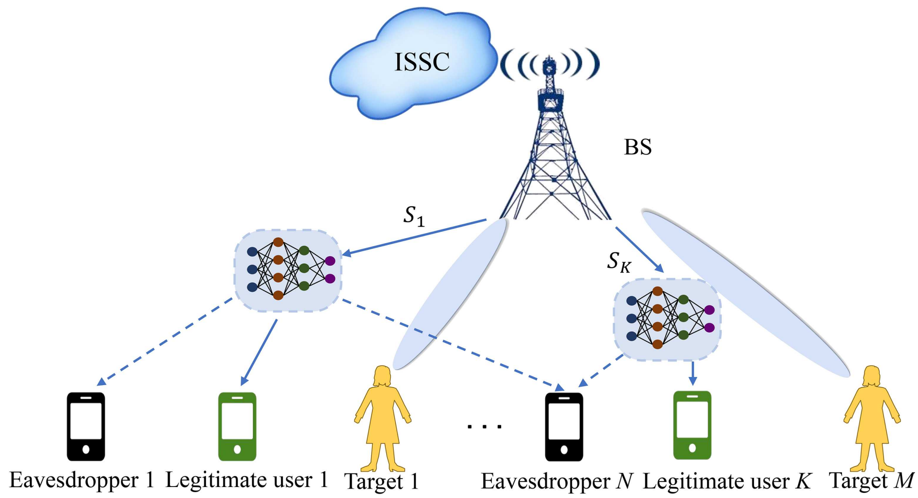

Figure 1 (Color online) Integrated sensing and semantic communication scenario with eavesdroppers.

through digital twin technology [32]. In [33], the authors have considered applying SC and sensing information transmission to metaverse scenarios.

Considering that the transmitted signal can also be used for sensing [34], therefore, we aim to investigate the secure resource allocation scheme in SC systems by considering both perfect CSI and imperfect CSI. Unlike conventional communication, in the ISSC system, this paper faces technical challenges in defining and processing the objective function, selecting optimization variables, and setting constraints. The specific contributions are as follows.

(1) Based on the ISSC system with multiple eavesdroppers, we first define SSR and further define SSE. We formulate the problem of maximizing SSE subject to constraints on secure communication and sensing performance under perfect and imperfect CSI.

(2) We transform the optimization problem into two subproblems, the beamforming optimization subproblem and the semantic parameter optimization subproblem. We iteratively solve the beamforming optimization subproblem by using the Dinkelbach algorithm, the successive convex approximation (SCA) method and the Bernstein-type inequality (BTI). Furthermore, we mathematically prove the monotonically decreasing property of SSE with respect to semantic parameters.

(3) The numerical results demonstrate the relationships between SSR, SSE and relevant parameters, indicating the effectiveness of the proposed secure resource allocation scheme. The simulation also validates that, under the same communication environment, the performance of SC is significantly better than conventional communication. For practical considerations, the system performance is superior when the eavesdroppers' CSI is imperfect compared to the case where CSI is perfect.

The organization of the paper is as indicated below. Section 2 introduces the system model. The optimization problem under perfect CSI and imperfect CSI are formulated in Sections 3 and 4 respectively, where we also propose a two-level iterative algorithm to solve the beamforming optimization subproblem and mathematically prove the relationship between SSE and semantic parameters for the semantic parameter optimization subproblem. Section 5 provides the simulation results, and finally, Section 6 sums up the conclusion.

2 System model

We consider a dual-functional BS equipped with an N_t-antennas uniform linear array (ULA) sends messages to K single-antenna users denoted by $\mathcal{K} = \{1, \ldots, K\}$, while sensing M radar targets denoted by $\mathcal{M} = \{1, \ldots, M\}$ in the ISSC system with N eavesdroppers denoted by $\mathcal{N} = \{1, \ldots, N\}$, as illustrated in Figure 1. The DeepSC system [35] is adopted as the SC model and installed at BS to carry out information transmission, where the transformer extracts the semantics effectively.

2.1 Communication model

In our model, a sentence is first generated at the BS, then it will be input into the DeepSC transmitter and transformed to a semantic symbol vector which can be transmitted over the wireless channel. On the user side, the received signal will first be decoded by the channel decoder, and then the semantic decoder will restore the sentence.

To be specific, the superimposed signal $\sum_{i\in\mathcal{K}}\boldsymbol{w}_i s_i$ is transmitted to all users from the BS, where $\boldsymbol{w}_i\in\mathbb{C}^{N_t\times 1}$ is beamforming vector for symbol s_i. Therefore, the received signal y_k at user k is given by

$$y_k=\boldsymbol{h}_k^{\mathrm{H}}\sum_{i\in\mathcal{K}}\boldsymbol{w}_i s_i+n_k=\sum_{i\in\mathcal{K}}\boldsymbol{h}_k^{\mathrm{H}}\boldsymbol{w}_i s_i+n_k, \tag{1}$$

where $\boldsymbol{h}_k=\Lambda_k^{-1/2}\widetilde{\boldsymbol{h}}_k,\forall k\in\mathcal{K}$ denotes the channel from the BS to user k, $\Lambda_k^{-1/2}$ and $\widetilde{\boldsymbol{h}}_k\in\mathbb{C}^{N_t\times 1}$ are the large and small scale fading, separately, and n_k denotes the circularly symmetric complex Gaussian noise with variance σ_n^2.

We adopt the semantic similarity [35] to evaluate the performance of the SC for text transmission. Then the semantic rate is designed as the quantity of semantic information effectively transmitted per second, with its unit being suts/s, which is as follows:

$$S=\frac{BI}{\tau L}\varepsilon(\tau,\gamma), \tag{2}$$

where τ represents the average number of semantic symbols for each word with its unit being symbols/word and γ denotes signal to interference plus noise ratio (SINR) for each user, which is measured in dBm. In (2), I (semantic units (suts)), L, B represent the average amount of semantic information encompassed in a sentence, the average number of words per sentence and bandwidth respectively. $\varepsilon(\tau,\gamma)$ represents the semantic similarity, which is defined as the degree of similarity between the semantic information recovered at the receiver and the original, unprocessed information at the transmitter [36]. It is used to measure the quality of SC services. Based on the system model, since the transmission of semantic signals relies on the DeepSC network architecture and channel conditions, the semantic similarity can be expressed as a function of the semantic parameter τ and the SINR [35].

Despite the importance of semantic rate as a key performance indicator for SCs, the theoretical exploration of SC design poses a challenge owing to the absence of a definitive expression for semantic similarity $\varepsilon(\tau,\gamma)$. To compensate for this limitation, we leverage the data regression method to approximate the semantic similarity with regard to γ for each τ. Specifically, the semantic similarity $\varepsilon(\tau,\gamma)$ is expected to exhibit an 'S' shape as a function of γ, spanning from $\varepsilon_{\min}$ to $\varepsilon_{\max}$. This observation prompts us to adopt the generalized logistic function as a tool to approximate $\varepsilon(\tau,\gamma)$, which is as follows:

$$\varepsilon(\tau,\gamma)\approx\widetilde{\varepsilon}(\tau,\gamma)\triangleq A_{\tau,1}+\frac{A_{\tau,2}-A_{\tau,1}}{1+\mathrm{e}^{-(C_{\tau,1}\gamma+C_{\tau,2})}}. \tag{3}$$

In (3), $A_{\tau,1},A_{\tau,2},C_{\tau,1},C_{\tau,2}$ are constant parameters. For any given τ, $A_{\tau,1}>0$ and $A_{\tau,2}>0$ limit the lower (left) and upper (right) bounds of the semantic similarity function, respectively, while $C_{\tau,1}>0$ represents the growth rate of the logistic function, and $C_{\tau,2}$ controls the logistic mid-point. Given that the symbol rate corresponds to the channel bandwidth of passband transmission, the overall semantic information transmitted over a channel with a bandwidth of B is equal to $BI/\tau L$ [35]. So that, we define $\boldsymbol{\tau}=(\tau_1,\ldots,\tau_k,\ldots,\tau_K)$ where τ_k represents the semantic parameter for user k and the achievable semantic rate at user k is

$$S_k=\frac{BI}{\tau_k L}\widetilde{\varepsilon}(\tau_k,\gamma_k), \tag{4}$$

where γ_k is expressed as

$$\gamma_k=\frac{\left|\boldsymbol{h}_k^{\mathrm{H}}\boldsymbol{w}_k\right|^2}{\sum_{i\in\mathcal{K},i\neq k}\left|\boldsymbol{h}_k^{\mathrm{H}}\boldsymbol{w}_i\right|^2+\sigma_n^2}. \tag{5}$$

Similarly, define $\boldsymbol{h}_{k,n}$ as the channel for eavesdropper n to decode signal transmitted to user k and the achievable semantic rate can be given as

$$S_{k,n}=\frac{BI}{\tau_k L}\widetilde{\varepsilon}(\tau_k,\gamma_{k,n}), \tag{6}$$

where $\gamma_{k,n}$ is expressed as

$$\gamma_{k,n} = \frac{\left|\boldsymbol{h}_{k,n}^{\mathrm{H}}\boldsymbol{w}_k\right|^2}{\sum_{i\in\mathcal{K},i\neq k}\left|\boldsymbol{h}_{k,n}^{\mathrm{H}}\boldsymbol{w}_i\right|^2+\sigma_n^2}. \tag{7}$$

We assume that the SSR is determined by the best achievable semantic rate at the eavesdropper and thereby the SSR at user k is given by

$$\mathrm{SSR}_k = \left[S_k - \max_{n\in\mathcal{N}} S_{k,n}\right]^+. \tag{8}$$

2.2 Sensing model

In the ISSC model, signals intended for communication can also be utilized to perform radar sensing tasks. We consider sensing N movable targets by first acquiring their position information through scanning, and subsequently conducting real-time monitoring and channel estimation of the sensing targets based on this position information. However, it is imperative to satisfy certain sensing requirements, including designing the covariance matrix for the transmitted signals, which is defined as

$$\boldsymbol{R}_{\boldsymbol{w}} = \sum_{k\in\mathcal{K}} \boldsymbol{w}_k\boldsymbol{w}_k^{\mathrm{H}}. \tag{9}$$

By acquiring target location information through scanning for real-time detection, facilitating channel estimation by sensing specific target locations (including eavesdroppers), and multiplexing communication signals as sensing signals for mutual cooperation and resource sharing, the ISSC system significantly enhances the overall efficiency and security of communication. Under the given location information of the targets, the sensing system aims to maximize the effective sensing power, which is defined as the power of the sensing signal in the directions of the targets and is expressed as

$$P(\theta_m) = \boldsymbol{a}^{\mathrm{H}}(\theta_m)\boldsymbol{R}_{\boldsymbol{w}}\boldsymbol{a}(\theta_m),\ \forall m\in\mathcal{M}. \tag{10}$$

In (10), θ_m represents the direction for target m, while its steering vector can be denoted as $\boldsymbol{a}(\theta_m) = [1, \mathrm{e}^{\mathrm{j}\frac{2\pi}{\lambda}d\sin(\theta_m)},\ldots,\mathrm{e}^{\mathrm{j}\frac{2\pi}{\lambda}d(N_t-1)\sin(\theta_m)}]^{\mathrm{T}}$, where λ and d refer to the carrier wavelength and antenna spacing, respectively. In this model, we assume that it is desirable to have the sensing power evenly distributed across different target directions, to make sure that each target can be detected in a fair and effective manner. Furthermore, the cross-correlation between the transmitted signals directed toward any two targets can be expressed as $C(\theta_k,\theta_p) = |\boldsymbol{a}^{\mathrm{H}}(\theta_k)\boldsymbol{R}_{\boldsymbol{w}}\boldsymbol{a}(\theta_p)|,\ \forall k\neq p\in\mathcal{M}$, which is supposed to be so low that adaptive location can be achieved by the sensing system. The mean-squared cross-correlation of the $\frac{M^2-M}{2}$ pairs of sensing targets is as follows:

$$\bar{C} = \frac{2}{M^2-M}\sum_{k=1}^{M-1}\sum_{p=k+1}^{M} C(\theta_k,\theta_p)^2. \tag{11}$$

2.3 CSI error model

One of the most important procedures for designing the communication system is acquiring CSI, which contains various attributes of the channel to describe the fading conditions during signal transmission. Most of the current research in communication assumes perfect CSI. Nevertheless, owing to various factors like hardware impairment and feedback delays, obtaining perfect CSI in practical scenarios is often challenging. Therefore, this paper investigates the secure resource allocation problem for the ISSC system both considering perfect and imperfect CSI scenarios. In general, there are two types of CSI errors: the bounded CSI error and the statistical CSI error, which are described as follows.

(1) Bounded CSI error:

$$\boldsymbol{h} = \hat{\boldsymbol{h}} + \triangle\boldsymbol{h}, \tag{12a}$$

$$|\triangle\boldsymbol{h}| \leqslant \epsilon_k. \tag{12b}$$

(2) Statistical CSI error:

$$\boldsymbol{h} = \hat{\boldsymbol{h}} + \triangle\boldsymbol{h}, \tag{13a}$$

$$\triangle\boldsymbol{h} \sim \mathcal{CN}(0, \boldsymbol{\Sigma}). \tag{13b}$$

In (12) and (13), $\hat{\boldsymbol{h}}$ denotes the estimates of $\boldsymbol{h}$ and $\triangle\boldsymbol{h}$ is the channel estimation errors.

3 Optimization with perfect CSI

In this section, all the CSI in the ISSC system is assumed to be known so perfectly that we adopt the SSE to measure the efficiency of the model, considering the constraints in communication and sensing.

3.1 Problem formulation

In the ISSC model, we aim to maximize the SSE which represents the ratio of the sum of SSRs to the total transmit power, while satisfying the relevant constraints in terms of secure communication and sensing. To solve the problem effectively, we adopt the expression of the SSR in the objective function. The resultant optimization problem is formulated as

$$\max_{\boldsymbol{w},\boldsymbol{\tau},p_t} \quad \frac{\sum_{k\in\mathcal{K}}[S_k - \max_{n\in\mathcal{N}} S_{k,n}]^+}{\sum_{k\in\mathcal{K}} \mathrm{tr}(\boldsymbol{w}_k\boldsymbol{w}_k^{\mathrm{H}})} \tag{14}$$

$$\text{s.t.} \quad \left[S_k - \max_{n\in\mathcal{N}} S_{k,n}\right]^+ \geqslant S_{\min,k},\ \forall k \in \mathcal{K}, \tag{14a}$$

$$|P(\theta_k) - P(\theta_p)| \leqslant P_{\mathrm{diff}},\ \forall k \neq p \in \mathcal{M}, \tag{14b}$$

$$\mathrm{diag}\left(\sum_{k\in\mathcal{K}} \boldsymbol{w}_k\boldsymbol{w}_k^{\mathrm{H}}\right) = \frac{p_t\mathbf{1}^{N_t\times 1}}{N_t}, \tag{14c}$$

$$\bar{C} \leqslant \xi, \tag{14d}$$

$$P(\theta_m) \geqslant P_D,\ \forall m \in \mathcal{M}, \tag{14e}$$

$$\tau_k \in \mathbb{N}^+,\ 1 \leqslant \tau_k \leqslant \tau_{\max},\ \forall k \in \mathcal{K}. \tag{14f}$$

Compared to conventional communication, this paper introduces metrics related to semantic, semantic variables, and constraints. In problem (14), Eq. (14a) is a secure communication constraint with threshold $S_{\min,k}$ that ensures secure SC while Eqs. (14b), (14d) and (14e) are radar target sensing constraints. Eq. (14c) is the transmit power constraint for each antenna, where p_t represents the total transmit power. To ensure that the BS can sense targets in different directions with similar signal levels, constraint (14b) requires that the difference in sensing signal power among different target directions be below a certain threshold, i.e., P_{diff}. Eq. (14d) guarantees that the mean-squared cross-correlation remains below a desired upper bound ξ. The constraint (14e) sets a requirement for the signal sensing capability, specifying that the sensing signal power in the target direction should be higher than the threshold P_D. The constraint (14f) restricts the range of values for the semantic parameter τ_k, specifying that it should take integer values between 1 and $\tau_{\max}$ inclusive. But obtaining the global optimal solution for problem (14) is still a highly challenging task because of the following two main reasons. First, The SSR's expression is neither convex nor concave, which results in the objective function being non-concave and the constraint (14a) being non-convex. Second, the quadratic form of the covariance matrix makes the constraints (14b) and (14c) non-convex. Therefore, the Dinkelbach method is utilized to simplify the objective function from the fractional form to a subtractive form, and then the optimization problem (14) can be transformed into a convex problem by introducing slack variables and the SCA method. Adopting convex optimization methods in this paper to solve the problem of optimizing security resource allocation is for that it can meet the needs of precise theoretical analysis and efficient resource utilization in complex communication and sensing tasks, and can also solve problems with limited data compared to ML methods.

3.2 Proposed solution

In this subsection, the above optimization problem (14), which is hard to be solved in a direct way, will be decoupled into two independent sub-optimization problems, i.e., beamforming optimization and semantic parameter optimization.

3.2.1 *Beamforming optimization*

Given the values of the semantic parameter $\boldsymbol{\tau}$, the optimization problem becomes the optimization of the beamforming vector. The constraint (14a) guarantees that $[S_k - \max_{n\in\mathcal{N}} S_{k,n}]^+$ is always greater than zero, therefore the numerator $[S_k - \max_{n\in\mathcal{N}} S_{k,n}]^+$ of the objective function is equivalent to $S_k - \max_{n\in\mathcal{N}} S_{k,n}$. We define $\widetilde{S}_{\min,k} = \frac{\tau_k L}{(A_{\tau,2}-A_{\tau,1})BI} S_{\min,k}$ and $\boldsymbol{W} = (\boldsymbol{W}_1,\ldots,\boldsymbol{W}_k,\ldots,\boldsymbol{W}_K)$, where $\boldsymbol{W}_k = \boldsymbol{w}_k\boldsymbol{w}_k^{\mathrm{H}}$. Since $C_{\tau,1}$ represents the growth rate of semantic similarity, and $C_{\tau,2}$ affects the changes in semantic similarity, without loss of generality, we set $C_{\tau,1} = \tau_k$ and $C_{\tau,2} = 0$. Besides, the values of $C_{\tau,1}$ and $C_{\tau,2}$ do not affect the conclusion of the research question [36]. Invoking slack variable φ_k to substitude $\max_{n\in\mathcal{N}} \gamma_{k,n}$ and letting $\boldsymbol{\varphi} = (\varphi_1,\ldots,\varphi_k,\ldots,\varphi_K)$, then we can transform optimization problem (14) into optimization problem (15) as follows:

$$
\begin{aligned}
\max_{\boldsymbol{W},p_t,\boldsymbol{\varphi}} \quad & \frac{\sum_{k\in\mathcal{K}}\left(\frac{1}{1+\mathrm{e}^{-\tau_k\gamma_k}} - \frac{1}{1+\mathrm{e}^{-\tau_k\varphi_k}}\right)}{\sum_{k\in\mathcal{K}} \mathrm{tr}(\boldsymbol{W}_k)} && (15)\\
\text{s.t.} \quad & \frac{1}{1+\mathrm{e}^{-\tau_k\gamma_k}} - \frac{1}{1+\mathrm{e}^{-\tau_k\varphi_k}} \geqslant \widetilde{S}_{\min,k},\ \forall k\in\mathcal{K}, && (15\mathrm{a})\\
& \varphi_k \geqslant \gamma_{k,n},\ \forall n\in\mathcal{N},\ \forall k\in\mathcal{K}, && (15\mathrm{b})\\
& |P(\theta_k) - P(\theta_p)| \leqslant P_{\mathrm{diff}},\ \forall k\neq p\in\mathcal{M}, && (15\mathrm{c})\\
& \mathrm{diag}\left(\sum_{k\in\mathcal{K}} \boldsymbol{W}_k\right) = \frac{p_t \boldsymbol{1}^{N_t\times 1}}{N_t}, && (15\mathrm{d})\\
& \bar{C} \leqslant \xi, && (15\mathrm{e})\\
& P(\theta_m) \geqslant P_D,\ \forall m\in\mathcal{M}, && (15\mathrm{f})\\
& \boldsymbol{W}_k \succeq 0,\ \boldsymbol{W}_k = \boldsymbol{W}_k^{\mathrm{H}},\ \forall k\in\mathcal{K}, && (15\mathrm{g})\\
& \mathrm{rank}(\boldsymbol{W}_k) = 1,\ \forall k\in\mathcal{K}. && (15\mathrm{h})
\end{aligned}
$$

Clearly, the problem (15) remains nonconvex due to the fractional nature of the objective function. Consequently, we incorporate the theorem outlined in [37] to address this issue.

Theorem 1. The optimal η^* of problem (15) can be obtained from the following optimization problem (16) if and only if $f(\eta^*) = 0$.

$$
\begin{aligned}
\max_{\boldsymbol{W},p_t,\boldsymbol{\varphi},\eta} \quad & \sum_{k\in\mathcal{K}}\left(\frac{1}{1+\mathrm{e}^{-\tau_k\gamma_k}} - \frac{1}{1+\mathrm{e}^{-\tau_k\varphi_k}}\right) - \eta\sum_{k\in\mathcal{K}} \mathrm{tr}(\boldsymbol{W}_k) && (16)\\
\text{s.t.} \quad & (15\mathrm{a})\text{–}(15\mathrm{h}).
\end{aligned}
$$

Proof. See Appendix A.

Based on Theorem 1, the fractional form of the objective function in (15) has been converted into the subtractive form of that in (16). Hence, our attention is directed towards the constrained optimization problem (16).

Even though the objective function has been changed from fractional form to subtractive form, the objective function still remains non-concave owing to the expression of γ_k and nonconcavity of $-\frac{1}{1+\mathrm{e}^{-\tau_k\varphi_k}}$. Hence, we introduce z_k to replace $\frac{1}{1+\mathrm{e}^{-\tau_k\gamma_k}}$ and define $\boldsymbol{z} = (z_1,\ldots,z_k,\ldots,z_K)$. We utilize the Taylor series expansion to approximate the concave function $\frac{1}{1+\mathrm{e}^{-\tau_k\varphi_k}}$, which is presented as follows:

$$
\frac{1}{1+\mathrm{e}^{-\tau_k\varphi_k}} \leqslant \frac{1}{1+\mathrm{e}^{-\tau_k\bar{\varphi}_k}} + \frac{\tau_k\mathrm{e}^{-\tau_k\bar{\varphi}_k}}{(1+\mathrm{e}^{-\tau_k\bar{\varphi}_k})^2}(\varphi_k - \bar{\varphi}_k). \tag{17}
$$

We define $T_{e_k}=\frac{1}{1+\mathrm{e}^{-\tau_k\bar{\varphi}_k}}+\frac{\tau_k\mathrm{e}^{-\tau_k\bar{\varphi}_k}}{(1+\mathrm{e}^{-\tau_k\bar{\varphi}_k})^2}(\varphi_k-\bar{\varphi}_k)$ and convert maximizing the original objective function to maximizing the lower bound of its maximum value, so that the problem (16) can be rewritten as

$$\max_{\boldsymbol{W},p_t,\boldsymbol{\varphi},\boldsymbol{z},\eta}\sum_{k\in\mathcal{K}}(z_k-T_{e_k})-\eta\sum_{k\in\mathcal{K}}\mathrm{tr}(\boldsymbol{W}_k) \tag{18}$$

$$\text{s.t.}\quad z_k-T_{e_k}\geqslant\widetilde{S}_{\min,k},\ \forall k\in\mathcal{K}, \tag{18a}$$

$$z_k\leqslant\frac{1}{1+\mathrm{e}^{-\tau_k\gamma_k}},\ \forall k\in\mathcal{K}, \tag{18b}$$

$$0\leqslant z_k\leqslant\frac{1}{2},\ \forall k\in\mathcal{K}, \tag{18c}$$

$$\text{(15b)–(15h).}$$

So far, the objective function for the problem (16) has been completely converted into a concave function, but problem (18) still remains a non-convex problem because of constraints (15b) and (18b).

For (15b), we define $\boldsymbol{H}_{k,n}\triangleq\boldsymbol{h}_{k,n}\boldsymbol{h}_{k,n}^{\mathrm{H}}$, then the constraint (15b) can be expanded as

$$\gamma_{k,n}=\frac{\mathrm{tr}(\boldsymbol{H}_{k,n}\boldsymbol{W}_k)}{\sum_{i\in\mathcal{K},i\neq k}\mathrm{tr}(\boldsymbol{H}_{k,n}\boldsymbol{W}_i)+\sigma_n^2}\leqslant\varphi_k,\ \forall k\in\mathcal{K}. \tag{19}$$

Taking the logarithm of both sides of the inequality, we have

$$\log_2\mathrm{tr}(\boldsymbol{H}_{k,n}\boldsymbol{W}_k)-\log_2\left(\sum_{i\in\mathcal{K},i\neq k}\mathrm{tr}(\boldsymbol{H}_{k,n}\boldsymbol{W}_i)+\sigma_n^2\right)-\log_2\varphi_k\leqslant 0,\ \forall k\in\mathcal{K}. \tag{20}$$

Since the nonconvexity of inequality (20) lies on the first term, a first-order Taylor expansion is applied to $\log_2\mathrm{tr}(\boldsymbol{H}_{k,n}\boldsymbol{W}_k)$ denoted as $T_{\varphi_k}=\log_2\mathrm{tr}(\boldsymbol{H}_{k,n}\bar{\boldsymbol{W}}_k)+\frac{1}{\ln 2\mathrm{tr}(\boldsymbol{H}_{k,n}\bar{\boldsymbol{W}}_k)}\mathrm{tr}\left[(\boldsymbol{H}_{k,n})^{\mathrm{T}}(\boldsymbol{W}_k-\bar{\boldsymbol{W}}_k)\right]$. Then the constraint (20) can be transformed into

$$T_{\varphi_k}-\log_2\left(\sum_{i\in\mathcal{K},i\neq k}\mathrm{tr}(\boldsymbol{H}_{k,n}\boldsymbol{W}_i)+\sigma_n^2\right)-\log_2\varphi_k\leqslant 0. \tag{21}$$

Similarly, we apply the equivalence transformation to the constraint (18b) and take the logarithm of both sides of the inequality as follows:

$$\log_2\left(\sum_{i\in\mathcal{K},i\neq k}\mathrm{tr}(\boldsymbol{H}_k\boldsymbol{W}_i)+\sigma_n^2\right)-\log_2\mathrm{tr}(\boldsymbol{H}_k\boldsymbol{W}_k)-\log_2\tau_k+\log_2\left(-\log\left(\frac{1}{z_k}-1\right)\right)\leqslant 0,\ \forall k\in\mathcal{K}. \tag{22}$$

The inequality (22) is still non-convex due to the first and last terms, so that we replace $-\log(\frac{1}{z_k}-1)$ with y_k and apply a first-order Taylor expansion to $\log_2\left(\sum_{i\in\mathcal{K},i\neq k}\mathrm{tr}(\boldsymbol{H}_k\boldsymbol{W}_i)+\sigma_n^2\right)$ and $\log_2 y_k$ expressed as T_{γ_k} and T_{y_k} respectively, which can be expressed as follows:

$$T_{\gamma_k}=\log_2\left(\sum_{i\in\mathcal{K},i\neq k}\mathrm{tr}(\boldsymbol{H}_k\bar{\boldsymbol{W}}_i)+\sigma_n^2\right)+\frac{\sum_{i\in\mathcal{K},i\neq k}\mathrm{tr}\left[(\boldsymbol{H}_k)^{\mathrm{T}}(\boldsymbol{W}_i-\bar{\boldsymbol{W}}_i)\right]}{\ln 2\left(\sum_{i\in\mathcal{K},i\neq k}\mathrm{tr}(\boldsymbol{H}_k\bar{\boldsymbol{W}}_i)+\sigma_n^2\right)}, \tag{23}$$

$$T_{y_k}=\log_2(\bar{y}_k)+\frac{1}{\ln 2\bar{y}_k}(y_k-\bar{y}_k). \tag{24}$$

Then, the inequality (22) can be transformed as

$$T_{\gamma_k}-\log_2\mathrm{tr}(\boldsymbol{H}_k\boldsymbol{W}_k)-\log_2\tau_k+T_{y_k}\leqslant 0,\ \forall k\in\mathcal{K}, \tag{25}$$

$$y_k\geqslant-\log\left(\frac{1}{z_k}-1\right),\ y_k\geqslant 0,\ \forall k\in\mathcal{K}. \tag{26}$$

Algorithm 1 Optimal beamforming for the SSE model.

Function: outer_iteration
Initialize $i = 0$ and $\eta^0 = 0$.
$\left|\eta^i - \eta^{i+1}\right| \leqslant \epsilon$, where ϵ is the tolerance.
(i) Call Function inner_iteration with η^i to obtain the optimal solution $(\boldsymbol{W}^i, p_t^i, \boldsymbol{\varphi}^i, \boldsymbol{z}^i, \boldsymbol{y}^i)$;
(ii) Update η^{i+1};
(iii) Let $i = i + 1$.
Obtain the maximum $\eta^* = \eta^i$ and the optimal $\boldsymbol{W}^* = \boldsymbol{W}^i$ for problem (16).
End
Function: inner_iteration
Initialize $i = 0$.
Find a feasible solution $(\boldsymbol{W}^0, p_t^0, \boldsymbol{\varphi}^0, \boldsymbol{z}^0, \boldsymbol{y}^0)$ for problem (28) and calculate f^0.
$\left|f^i - f^{i+1}\right| \leqslant \epsilon$, where ϵ is the tolerance.
(i) Find the optimal $(\boldsymbol{W}^{i+1}, p_t^{i+1}, \boldsymbol{\varphi}^{i+1}, \boldsymbol{z}^{i+1}, \boldsymbol{y}^{i+1})$ of problem (28) for obtained $(\boldsymbol{W}^i, p_t^i, \boldsymbol{\varphi}^i, \boldsymbol{z}^i, \boldsymbol{y}^i)$ and η;
(ii) Calculate f^{i+1};
(iii) Let $i = i + 1$.
Gaussian randomization is used to reconstruct the optimal solution satisfying the rank-one constraint.
End

The transformation of inequality (26) is given by

$$z_k - \frac{1}{1 + \mathrm{e}^{-y_k}} \leqslant 0, \ y_k \geqslant 0, \ \forall k \in \mathcal{K}. \tag{27}$$

Clearly, the inequality (27) is convex. Therefore, based on (21), (25) and (27), the optimization problem can ultimately be transformed as follows:

$$\max_{\boldsymbol{W}, p_t, \boldsymbol{\varphi}, \boldsymbol{z}, \boldsymbol{y}, \eta} \sum_{k \in \mathcal{K}} (z_k - T_{e_k}) - \eta \sum_{k \in \mathcal{K}} \mathrm{tr}(\boldsymbol{W}_k) \tag{28}$$

$$\text{s.t.} \quad T_{\varphi_k} - \log_2 \left(\sum_{i \in \mathcal{K}, i \neq k} \mathrm{tr}(\boldsymbol{H}_{k,n} \boldsymbol{W}_i) + \sigma_n^2 \right) - \log_2 \varphi_k \leqslant 0, \ \forall k \in \mathcal{K}, \tag{28a}$$

$$T_{\gamma_k} - \log_2 \mathrm{tr}(\boldsymbol{H}_k \boldsymbol{W}_k) - \log_2 \tau_k + T_{y_k} \leqslant 0, \tag{28b}$$

$$z_k - \frac{1}{1 + \mathrm{e}^{-y_k}} \leqslant 0, \ y_k \geqslant 0, \ \forall k \in \mathcal{K}, \tag{28c}$$

$$\text{(15c)–(15h), (18a).}$$

So far, the optimization problem (28) can be addressed through the application of standard convex optimization technique if the rank-one constraint (15h) were disregarded, can be addressed through Gaussian randomization. Regarding this optimization problem, a two-level iterative algorithm is put forward to obtain the optimal beamforming for the SSE problem as summarized in Algorithm 1. The convergence characteristics of the outer iteration, utilizing the golden search method, have been extensively studied and well documented [37] and that of the inner iteration can be ensured by Theorem 2.

Theorem 2. The iteration of the proposed algorithm generates a sequence of feasible solutions that ascend and eventually converge to the optimal solution of (28).

Proof. See Appendix B.

Computational complexity. The computational complexity of the suggested algorithm is contingent upon the number of iterations, the variable size, as well as the constraints imposed during the outer and inner iterations. Based on the given tolerance ϵ, the complexity of the iterations without convex programming is given by

$$\mathcal{O}\left(\log \left(\frac{\eta^{\mathrm{up}}}{\epsilon} \right) \log \left(\frac{f^{\mathrm{up}}}{\epsilon} \right) \right), \tag{29}$$

where $\eta^{\mathrm{up}} = f^{\mathrm{up}} = \sum_{k \in \mathcal{K}} \frac{1}{1 + \mathrm{e}^{-\tau_k \frac{p_t \mathrm{tr}(H_k)}{N}}}$. For given $N_t + 1$ scalar variable in (28), the interior point method needs at most $\mathcal{O}((N_t + 1) \log(1/\epsilon))$ calculations at each inner iteration. Finally, the computational complexity under the worst case can be approximately expressed as

$$\mathcal{O}(\log^3(1/\epsilon) N_t^3). \tag{30}$$

3.2.2 *Semantic parameter optimization*

Given optimization variables $\boldsymbol{w}_k$, the optimization problem (14) can be transformed into

$$\max_{\boldsymbol{\tau}} \quad \frac{\sum_{k\in\mathcal{K}}[S_k - \max_{n\in\mathcal{N}} S_{k,n}]^+}{\sum_{k\in\mathcal{K}} \mathrm{tr}(\boldsymbol{w}_k\boldsymbol{w}_k^{\mathrm{H}})} \tag{31}$$

$$\text{s.t.} \quad \left[S_k - \max_{n\in\mathcal{N}} S_{k,n}\right]^+ \geqslant S_{\min,k},\ \forall k\in\mathcal{K}, \tag{31a}$$

$$\tau_k \in \mathbb{N}^+,\ \tau_{\min} \leqslant \tau_k \leqslant \tau_{\max},\ \forall k\in\mathcal{K}. \tag{31b}$$

Maximizing the sum of SSE in the problem (31) can be equivalent to the problem of maximizing the SSE of a single user. In addition, since the optimization variable beamforming vector $\boldsymbol{w}_k$ is a given value, we set $\varphi_k = \max_{n\in\mathcal{N}} \gamma_{n,k}$ and maximize the numerator of the objective function. Maximing $S_k - \max_{n\in\mathcal{N}} S_{k,n}$ is inevitably satisfying the constant (31a), thus, the optimization problem can be converted into

$$\max_{\tau_k} \quad \frac{1}{\tau_k}\left(\frac{1}{1+\mathrm{e}^{-\tau_k\gamma_k}} - \frac{1}{1+\mathrm{e}^{-\tau_k\varphi_k}}\right) \tag{32}$$

$$\text{s.t.} \quad \tau_k \in \mathbb{N}^+,\ \tau_{\min} \leqslant \tau_k \leqslant \tau_{\max},\ \forall k\in\mathcal{K}. \tag{32a}$$

Utilizing Theorem 3, that the objective function is monotonically decreasing about the semantic parameter τ_k can be demonstrated.

Theorem 3. $\frac{1}{\tau_k}(\frac{1}{1+\mathrm{e}^{-\tau_k\gamma_k}} - \frac{1}{1+\mathrm{e}^{-\tau_k\varphi_k}})$ is monotonically decreasing with respect to τ_k, and the optimal solution for (32) can be taken as the left endpoint value of the domain.

Proof. See Appendix C.

In conclusion, the objective function in the optimization problem (31) is a monotonically decreasing function about $\boldsymbol{\tau}$, and the optimal solution can be taken as the left endpoint value of the domain.

4 Optimization with imperfect CSI

To achieve the optimal SSE, we assume that perfect channel condition could be obtained, however, the perfect CSIs of users and eavesdroppers are quite difficult to obtain. Hence, we contemplate the statistical CSI error for the channel from the BS to eavesdroppers for that it is more intricately linked to channel estimation error. We assume the channel $\boldsymbol{h}_{k,n}$ is imperfect, which is given by

$$\boldsymbol{h}_{k,n} = \hat{\boldsymbol{h}}_{k,n} + \triangle\boldsymbol{h}_{k,n}, \tag{33}$$

where $\hat{\boldsymbol{h}}_{k,n}$ denotes the estimate of $\boldsymbol{h}_{k,n}$, which can be obtained through training pilot which is transmitted by all eavesdroppers. $\triangle\boldsymbol{h}_{k,n}$ is the channel estimation errors for eavesdropper n, which is modeled to follow circularly symmetric complex gaussian $\mathcal{CN}(0,\boldsymbol{\Sigma}_{k,n})$, and $\boldsymbol{\Sigma}_{k,n}$ is the semidefinite error covariance matrix.

4.1 Problem formulation

In this subsection, we consider the case that the CSI of eavesdroppers is imperfect. Under imperfect CSI conditions, the eavesdropper's semantic rate follows a certain probability distribution, so we establish a maximum threshold for the eavesdropper's semantic rate, denoted as S_e, to compute the SSR while ensuring communication. However, the secrecy outrage probability of per-eavesdropper has to be considered. Therefore, the optimization problem to maximize the SSE can be rewritten as

$$\max_{\boldsymbol{w},p_t,\boldsymbol{\tau}} \quad \frac{\sum_{k\in\mathcal{K}}[S_k - S_e]^+}{\sum_{k\in\mathcal{K}} \mathrm{tr}(\boldsymbol{w}_k\boldsymbol{w}_k^{\mathrm{H}})} \tag{34}$$

$$\text{s.t.} \quad |P(\theta_k) - P(\theta_p)| \leqslant P_{\mathrm{diff}},\ \forall k \neq p \in \mathcal{M}, \tag{34a}$$

$$\mathrm{diag}\left(\sum_{k\in\mathcal{K}} \boldsymbol{w}_k\boldsymbol{w}_k^{\mathrm{H}}\right) = \frac{p_t\mathbf{1}^{N_t\times 1}}{N_t}, \tag{34b}$$

$$\bar{C} \leqslant \xi, \tag{34c}$$

$$P(\theta_m) \geqslant P_D,\ \forall m \in \mathcal{M}, \tag{34d}$$

$$\tau_k \in \mathbb{N}^+,\ 1 \leqslant \tau_k \leqslant \tau_{\max},\ \forall k \in \mathcal{K}, \tag{34e}$$

$$[S_k - S_e]^+ \geqslant S_{\min,k},\ \forall k \in \mathcal{K}, \tag{34f}$$

$$\mathrm{Pr}_{h_{k,n}} \left\{ \max_{n \in \mathcal{N}} S_{k,n} \leqslant S_e \right\} \geqslant 1 - \rho_k. \tag{34g}$$

For the constraint (34f), due to that S_e is the maximum threshold for the eavesdropper's semantic rate, Eq. (34f) can be rewritten as $S_k \geqslant S_u$, where $S_u = S_e + S_{\min,k}$. So that problem (34) can be transformed as

$$\max_{\boldsymbol{w}, p_t, \boldsymbol{\tau}} \ \frac{\sum_{k \in \mathcal{K}} [S_k - S_e]^+}{\sum_{k \in \mathcal{K}} \mathrm{tr}(\boldsymbol{w}_k \boldsymbol{w}_k^{\mathrm{H}})} \tag{35}$$

$$\text{s.t.}\ \ |P(\theta_k) - P(\theta_p)| \leqslant P_{\text{diff}},\ \forall k \neq p \in \mathcal{M}, \tag{35a}$$

$$\mathrm{diag}\left(\sum_{k \in \mathcal{K}} \boldsymbol{w}_k \boldsymbol{w}_k^{\mathrm{H}} \right) = \frac{p_t \mathbf{1}^{N_t \times 1}}{N_t}, \tag{35b}$$

$$\bar{C} \leqslant \xi, \tag{35c}$$

$$P(\theta_m) \geqslant P_D,\ \forall m \in \mathcal{M}, \tag{35d}$$

$$\tau_k \in \mathbb{N}^+,\ 1 \leqslant \tau_k \leqslant \tau_{\max},\ \forall k \in \mathcal{K}, \tag{35e}$$

$$S_k \geqslant S_u,\ \forall k \in \mathcal{K}, \tag{35f}$$

$$\mathrm{Pr}_{h_{k,n}} \left\{ \max_{n \in \mathcal{N}} S_{k,n} \leqslant S_e \right\} \geqslant 1 - \rho_k. \tag{35g}$$

In the problem (35), except the same constraints in the problem (14), the constraint (35a) is the data rate requirement for user k and Eq. (35g) can be considered as the constraint of secrecy outage probability for eavesdropper n.

4.2 Proposed solution

4.2.1 *Beamforming optimization*

Under the given semantic parameter $\boldsymbol{\tau}$, due to the monotonically increasing property of semantic similarity $\varepsilon(\tau, \gamma)$ with respect to γ and fixed value S_e, problem (35) can be equivalent to

$$\max_{\boldsymbol{W}, p_t} \ \frac{\sum_{k \in \mathcal{K}} \frac{1}{1+\mathrm{e}^{-\tau_k \gamma_k}}}{\sum_{k \in \mathcal{K}} \mathrm{tr}(\boldsymbol{W}_k)} \tag{36}$$

$$\text{s.t.}\ \ |P(\theta_k) - P(\theta_p)| \leqslant P_{\text{diff}},\ \forall k \neq p \in \mathcal{M}, \tag{36a}$$

$$\mathrm{diag}\left(\sum_{k \in \mathcal{K}} \boldsymbol{W}_k \right) = \frac{p_t \mathbf{1}^{N_t \times 1}}{N_t}, \tag{36b}$$

$$\bar{C} \leqslant \xi, \tag{36c}$$

$$P(\theta_m) \geqslant P_D,\ \forall m \in \mathcal{M}, \tag{36d}$$

$$\boldsymbol{W}_k \succeq 0,\ \boldsymbol{W}_k = \boldsymbol{W}_k^{\mathrm{H}},\ \forall k \in \mathcal{K}, \tag{36e}$$

$$\mathrm{rank}(\boldsymbol{W}_k) = 1,\ \forall k \in \mathcal{K}, \tag{36f}$$

$$\gamma_k \geqslant \gamma_u, \tag{36g}$$

$$\mathrm{Pr}_{h_{k,n}} \{ \varphi_k \leqslant \gamma_e \} \geqslant 1 - \rho_k, \tag{36h}$$

where $\varphi_k = \max_{n \in \mathcal{N}} \gamma_{k,n}$, γ_u, γ_e and ρ_k are constants. By using Theorem 1, we transform the fractional form of the objective function in problem (36) into a subtractive form. For the constraint (36h), $\varphi_k = \max_{n \in \mathcal{N}} \gamma_{k,n} \leqslant \gamma_e$ is equivalent to $\gamma_{k,n} \leqslant \gamma_e$. Therefore, considering the analysis above, the optimization problem (36) can be rewritten as

$$\max_{\boldsymbol{W}, p_t, \eta} \sum_{k \in \mathcal{K}} \frac{1}{1 + \mathrm{e}^{-\tau_k \gamma_k}} - \eta \sum_{k \in \mathcal{K}} \mathrm{tr}(\boldsymbol{W}_k) \tag{37}$$

$$\text{s.t. } \Pr_{h_{k,n}}\{\gamma_{k,n} \leqslant \gamma_e\} \geqslant 1 - \rho_k, \tag{37a}$$
$$\text{(36a)–(36g)}.$$

Obviously, the problem (37) is still non convex because of the first term $\frac{1}{1+\mathrm{e}^{-\tau_k \gamma_k}}$ in the objective function and the constraints (36g) and (37a).

For objective function, by invoking slack variable z_k to substitute $\frac{1}{1+\mathrm{e}^{-\tau_k \gamma_k}}$ and denoting $\boldsymbol{z} = (z_1, \ldots, z_k, \ldots, z_K)$, the optimization problem (37) can be written as

$$\max_{\boldsymbol{W}, p_t, \boldsymbol{z}, \eta} \sum_{k\in\mathcal{K}} z_k - \eta \sum_{k\in\mathcal{K}} \mathrm{tr}(\boldsymbol{W}_k) \tag{38}$$
$$\text{s.t. } z_k \leqslant \frac{1}{1+\mathrm{e}^{-\tau_k \gamma_k}}, \ \forall k \in \mathcal{K}, \tag{38a}$$
$$\text{(36a)–(36g), (37a)}.$$

For (38a), we apply the equivalence transformation to it and take the logarithm of both sides of the inequality as follows:

$$\log_2\left(\sum_{i\in\mathcal{K}, i\neq k} \mathrm{tr}(\boldsymbol{H}_k \boldsymbol{W}_i) + \sigma_n^2\right) - \log_2 \mathrm{tr}(\boldsymbol{H}_k \boldsymbol{W}_k) - \log_2 \tau_k + \log_2\left(-\log\left(\frac{1}{z_k} - 1\right)\right) \leqslant 0, \ \forall k \in \mathcal{K}. \tag{39}$$

The inequality (39) is still non-convex due to the first and last terms, so we replace $-\log(\frac{1}{z_k} - 1)$ with y_k and apply a first-order Taylor expansion to $\log_2\left(\sum_{i\in\mathcal{K}, i\neq k} \mathrm{tr}(\boldsymbol{H}_k \boldsymbol{W}_i) + \sigma_n^2\right)$ and $\log_2 y_k$ expressed as T_{γ_k} and T_{y_k}, whose expressions have been shown above. Then, the inequality (39) can be transformed as

$$T_{\gamma_k} - \log_2 \mathrm{tr}(\boldsymbol{H}_k \boldsymbol{W}_k) - \log_2 \tau_k + T_{y_k} \leqslant 0, \ \forall k \in \mathcal{K}, \tag{40}$$

$$z_k - \frac{1}{1+\mathrm{e}^{-y_k}} \leqslant 0, \ y_k \geqslant 0, \ \forall k \in \mathcal{K}. \tag{41}$$

For (36g), it can be simplified as follows:

$$\gamma_k = \frac{\left|\boldsymbol{h}_k^{\mathrm{H}} \boldsymbol{w}_k\right|^2}{\sum_{i\in\mathcal{K}, i\neq k} \left|\boldsymbol{h}_k^{\mathrm{H}} \boldsymbol{w}_i\right|^2 + \sigma_n^2} \geqslant \gamma_u, \tag{42a}$$

$$\Leftrightarrow \boldsymbol{h}_k^{\mathrm{H}} \left(\boldsymbol{W}_k - \gamma_u \sum_{i\in\mathcal{K}, i\neq k} \boldsymbol{W}_i\right) \boldsymbol{h}_k \geqslant \gamma_u \sigma_n^2. \tag{42b}$$

Subsequently, we rephrase the per-eavesdropper secrecy outage probability (37a) which poses challenges due to the complexity of the SINR expression and the probability constraints. We initially simplify the SINR inequality, and subsequently, transform the probabilistic constraint into the deterministic constraint by leveraging Lemma 1 [38].

Lemma 1. Let $\triangle \boldsymbol{h}_{k,n} = \boldsymbol{\Sigma}_{k,n}^{1/2} \boldsymbol{v}_{k,n}$ denote the CSI error $\triangle \boldsymbol{h}_{k,n}$, where $\boldsymbol{v}_{k,n} \sim \mathcal{CN}(\boldsymbol{0}, \boldsymbol{I})$, $\boldsymbol{\Sigma}_{k,n} = \boldsymbol{\Sigma}_{k,n}^{1/2} \boldsymbol{\Sigma}_{k,n}^{1/2}$ and $(\boldsymbol{\Sigma}_{k,n}^{1/2})^{\mathrm{H}} = \boldsymbol{\Sigma}_{k,n}^{1/2}$, the constraint (37a) can be rewritten as

$$\begin{cases} \mathrm{tr}(\boldsymbol{A}_{k,n}) - \sqrt{-2\ln(\rho_{k,n})} p_{k,n} + \ln(\rho_{k,n}) q_{k,n} + c_{k,n} \geqslant 0, \\ \left\| \begin{bmatrix} \mathrm{vec}(\boldsymbol{A}_{k,n}) \\ \sqrt{2} \boldsymbol{u}_{k,n} \end{bmatrix} \right\|_2 \leqslant p_{k,n}, \\ q_{k,n} \boldsymbol{I} + \boldsymbol{A}_{k,n} \succeq 0, \ q_{k,n} \geqslant 0. \end{cases} \tag{43}$$

Proof. See Appendix D.

Hence, the optimization problem can be finally transformed as follows:

$$\max_{\boldsymbol{W}, p_t, \boldsymbol{z}, \boldsymbol{y}, \boldsymbol{p}, \boldsymbol{q}, \eta} \sum_{k\in\mathcal{K}} z_k - \eta \sum_{k\in\mathcal{K}} \mathrm{tr}(\boldsymbol{W}_k) \tag{44}$$

$$\text{s.t.} \quad T_{\gamma_k} - \log_2 \operatorname{tr}(\boldsymbol{H}_k \boldsymbol{W}_k) - \log_2 \tau_k + T_{y_k} \leqslant 0,\ \forall k \in \mathcal{K}, \tag{44a}$$

$$z_k - \frac{1}{1+\mathrm{e}^{-y_k}} \leqslant 0,\ y_k \geqslant 0,\ \forall k \in \mathcal{K}, \tag{44b}$$

$$\boldsymbol{h}_k^{\mathrm{H}} \left(\boldsymbol{W}_k - \gamma_u \sum_{i \in \mathcal{K}, i \neq k} \boldsymbol{W}_i \right) \boldsymbol{h}_k \geqslant \gamma_u \sigma_n^2, \tag{44c}$$

$$\operatorname{tr}(\boldsymbol{A}_{k,n}) - \sqrt{-2\ln(\rho_{k,n}) p_{k,n}} + \ln(\rho_{k,n}) q_{k,n} + c_{k,n} \geqslant 0, \tag{44d}$$

$$\left\| \begin{bmatrix} \operatorname{vec}(\boldsymbol{A}_{k,n}) \\ \sqrt{2}\boldsymbol{u}_{k,n} \end{bmatrix} \right\|_2 \leqslant p_{k,n}, \tag{44e}$$

$$q_{k,n}\boldsymbol{I} + \boldsymbol{A}_{k,n} \succeq 0,\ q_{k,n} \geqslant 0, \tag{44f}$$

$$\text{(36a)–(36f)}.$$

Obviously, the SSE optimization problem can be addressed through the application of the standard convex optimization technique if the rank-one constraint (36f) is disregarded. Regarding this optimization problem, the two-level iterative algorithm is also adopted to acquire the optimal beamforming for the SSE problem as summarized in Algorithm 1.

4.2.2 *Semantic parameter optimization*

Under the given optimization variable $\boldsymbol{w}_k$, the optimization problem (34) can be reformulated as

$$\max_{\boldsymbol{\tau}} \quad \frac{\sum_{k \in \mathcal{K}} [S_k - S_e]^+}{\sum_{k \in \mathcal{K}} \operatorname{tr}(\boldsymbol{w}_k \boldsymbol{w}_k^{\mathrm{H}})} \tag{45}$$

$$\text{s.t.} \quad \tau_k \in \mathbb{N}^+,\ \tau_{\min} \leqslant \tau_k \leqslant \tau_{\max},\ \forall k \in \mathcal{K}. \tag{45a}$$

Due to the given $\boldsymbol{w}_k$ and the expression of the data rate S_k, the problem (38) can be rewritten as

$$\max_{\tau_k} \quad \frac{1}{\tau_k} \frac{1}{1+\mathrm{e}^{-\tau_k \gamma_k}} \tag{46}$$

$$\text{s.t.} \quad \tau_k \in \mathbb{N}^+,\ \tau_{\min} \leqslant \tau_k \leqslant \tau_{\max},\ \forall k \in \mathcal{K}. \tag{46a}$$

We define the objective function as $f(\tau_k)$ and take the first derivative of it:

$$\frac{\mathrm{d}f(\tau_k)}{\mathrm{d}\tau_k} = \frac{\mathrm{e}^{\tau_k \gamma_k}(\tau_k \gamma_k - \mathrm{e}^{\tau_k \gamma_k} - 1)}{\left(\tau_k(\mathrm{e}^{\tau_k \gamma_k} + 1)\right)^2}. \tag{47}$$

Define $g(\tau_k) = \tau_k \gamma_k - \mathrm{e}^{\tau_k \gamma_k} - 1$ and its first derivative is given by

$$\frac{\mathrm{d}g(\tau_k)}{\mathrm{d}\tau_k} = \gamma_k(1 - \mathrm{e}^{\tau_k \gamma_k}). \tag{48}$$

Since τ_k is definitely greater than zero, $g(\tau_k)$ is a monotonically decreasing function, thereby $g(\tau_k) \leqslant g(0) = -2$, which demonstrates that $f(\tau_k)$, i.e., the objective function is a monotonically decreasing function about τ_k.

In conclusion, the objective function of the optimization problem (45) is monotonically decreasing with respect to $\boldsymbol{\tau}$, and the optimal solution can be taken as the left endpoint value of the domain.

5 Numerical results

In this section, the numerical findings demonstrate the convergence of the proposed algorithm in both perfect CSI and imperfect CSI scenarios, as well as the relationships between SSR, SSE and relevant parameters, respectively. This paper considers a BS equipped with $N_t = 4$ antennas that serve $K = 4$ single-antenna users for SC, while performing sensing tasks for $M = 2$ sensing targets. Additionally, there are $N = 5$ eavesdroppers near the BS simultaneously intercepting the data of the users. Unless specified

Table 1 Simulation parameters.

Parameter	Value
BS antennas	$N_t = 4$
Number of users	$K = 4$
Number of sensing targets	$M = 2$
Number of eavesdroppers	$N = 5$
Noise power	$\sigma^2 = -120$ dBm
Average semantic information in a word	$I/L = 1$ suts/word

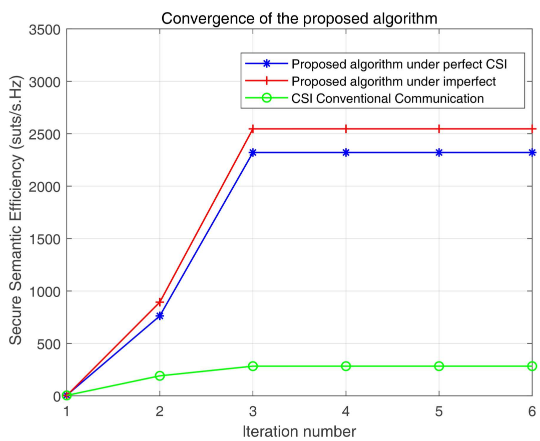

Figure 2 (Color online) Convergence of the proposed algorithm under both perfect CSI and imperfect CSI and conventional communication.

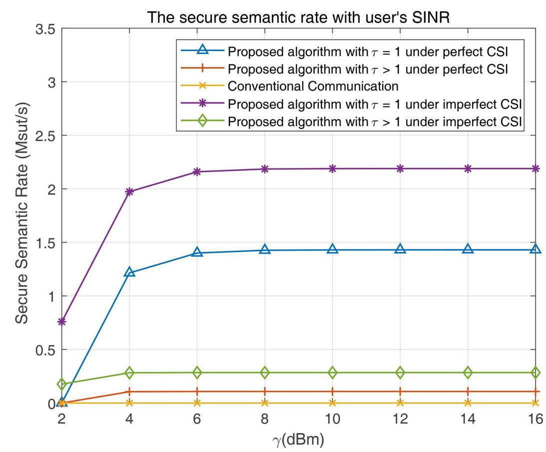

Figure 3 (Color online) SSR versus SINR.

otherwise, the remaining parameters are configured as follows: $\sigma_n^2 = 10^{-3}$, $I/L = 1$. The parameters used in the aforementioned simulations are presented in Table 1.

The convergence of the algorithm under perfect and imperfect CSI conditions and conventional communication is investigated in Figure 2. In this paper, the semantic parameter τ represents the average number of semantic symbols for each word, with its unit being symbols per word. We set $\tau = [1 : 10]$, when τ takes integer values less than 10, such as $\tau = 2$ or $\tau = 8$, the BS extracts and transmits partial semantic information. Since traditional communication transmits the source information in its entirety, the system operates in traditional communication mode when $\tau = 10$. As illustrated above, it is highly likely that the proposed algorithm under imperfect CSI converges with fewer iterations than that under perfect CSI, which is significantly fewer than that of conventional communication. In imperfect CSI scenario, where channel estimation errors are considered for the channels between the BS and the eavesdroppers, the convergence value of the objective function SSE is higher than that in the case of perfect CSI and conventional communication. In the imperfect CSI scenario, due to the statistical CSI errors in the eavesdropper's channel, the eavesdropper's semantic rate follows a certain probability distribution and the SSE under perfect CSI and imperfect CSI scheme is not comparable. We used a relatively small value for the probability ρ_k, thereby obtaining smaller parameter S_e, leading to a situation where the SSE under imperfect CSI conditions is higher than that under perfect CSI conditions.

Under the given upper and lower bounds of semantic similarity $A_{\tau,1} = 3$ and $A_{\tau,2} = 6$, Figure 3 analyses the relationships between the SSR and γ of users for different τ under the cases of perfect CSI and imperfect CSI, where the communication model takes $\tau = 10$ due to the conventional communication transmits the whole symbols of the sentence. From the Figure 3, as can be seen, the SSR of the SC increases with the increase of γ and eventually approaches a stable value. Meanwhile, the values for imperfect CSI case are greatly higher than that for perfect CSI, which are both evidently higher than that of conventional communication. Based on the expressions of SSR and SSE, both SSE and SSR are monotonically decreasing with respect to the semantic parameter τ. When $\tau = 10$, i.e., conventional communication, SSR and SSE approach 0.

In Figure 4, it can be directly observed that the SSR under imperfect CSI is significantly higher than that under perfect CSI, and the SSR shows a decreasing trend with respect to the semantic parameter τ.

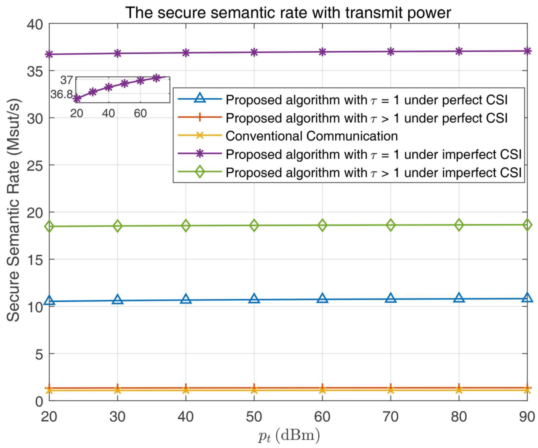

Figure 4 (Color online) SSR versus p_t.

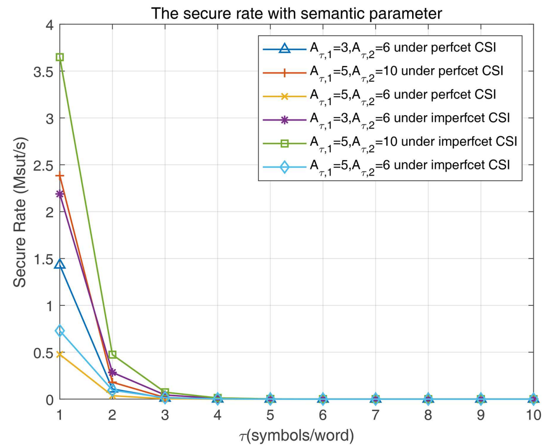

Figure 5 (Color online) SSR versus τ.

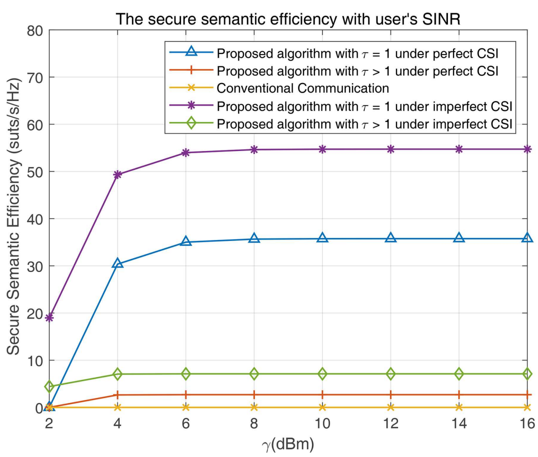

Figure 6 (Color online) SSE versus SINR.

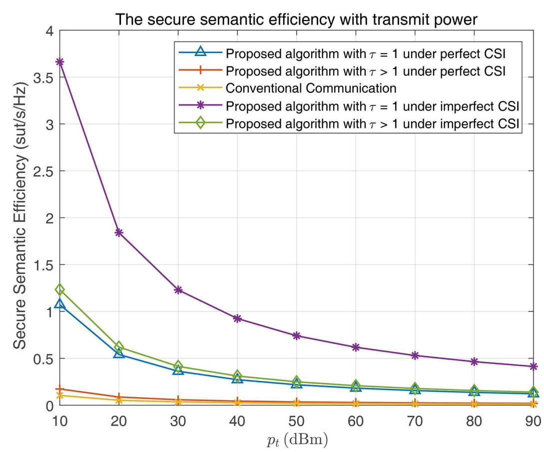

Figure 7 (Color online) SSE versus p_t.

Figure 4 presents an increasing trend of SSR with the transmit power p_t, however, this increasing trend is not very significant. In Figure 4, due to the large span of values taken by the horizontal axis p_t, the growth in the vertical axis, which represents the SSR, is not apparent relative to changes in the transmit power p_t. In fact, the SSR is positively correlated with the transmit power p_t, meaning that the SSR increases as the transmit power increases.

Figure 5 shows the relationships between the SSR and semantic parameter τ for different values of $A_{\tau,1}$ and $A_{\tau,2}$, i.e., the upper and lower asymptotes of semantic similarity. In Figure 5, overall, as previously demonstrated, the SSR decreases with the increase of the semantic parameter τ and the SSR under imperfect CSI is totally higher than that of perfect CSI. Specifically, the SSR decreases as $A_{\tau,1}$ increases under the given $A_{\tau,2}$ until it approaches zero infinitely, and increases as $A_{\tau,2}$ increases under the given $A_{\tau,1}$, which can be clearly observed that the greater the gap between the $A_{\tau,1}$ and $A_{\tau,2}$ the larger the SSR is.

Similar to Figure 3, under the given parameters, Figure 6 reveals the relationships between the SSE and users' γ. In Figure 6, the SSE increases both under perfect CSI and imperfect CSI with the increases of SINR, i.e., γ of users until a stable value, where the performance under imperfect CSI is better than that under perfect CSI, while the performance in SC scenario is significantly better than that in conventional communication scenario.

Figure 7 depicts the variation trend of SSE with respect to the transmit power p_t. As depicted in Figure 7, the SSE shows a decreasing trend with p_t and eventually converges to a stable value, indicating that SC demonstrates its advantages more prominently in environments with poor communication conditions. The SSE in the imperfect CSI scenario outperforms that in the perfect CSI scenario, and significantly surpasses the SSE in conventional communication scenarios. Furthermore, Figure 7 also verifies the

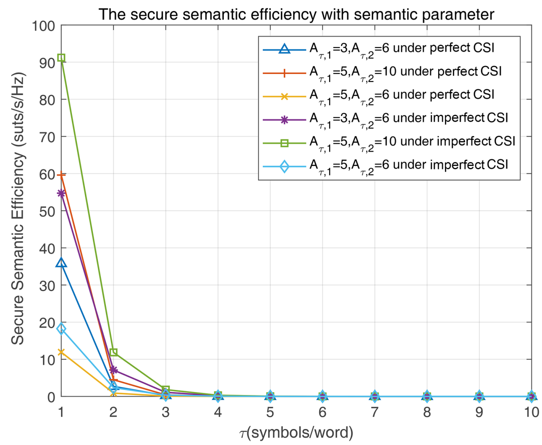

Figure 8 (Color online) SSE versus τ.

monotonically decreasing relationship between SSE and the semantic parameter τ.

In Figure 8, it becomes apparent that the SSE monotonically decreases as $A_{\tau,1}$ increases under the given $A_{\tau,2}$. Meanwhile, the lower the semantic parameter τ is, the higher the SSE will be until reaching its maximum value at $\tau = 1$. On the contrary, the SSE increases as the upper bound $A_{\tau,2}$ increases. Moreover, it is easily observed that the SSE will become higher with the increase of the gap between the upper and lower bounds of semantic similarity, i.e., $A_{\tau,2} - A_{\tau,1}$.

6 Conclusion

In this paper, we proposed a secure resource allocation scheme for the ISSC system under both perfect CSI and imperfect CSI which considers uncertainty for the channel from BS to eavesdroppers. We formulated the problem of maximizing SSE compliant with constraints on secure communication and sensing. The Dinkelbach algorithm, SCA method and the BTI are employed to transform the optimization problem into a convex problem. Then, the monotonically decreasing property of SSE with respect to semantic parameter τ is proved mathematically. The simulation results further validate the practicality of the secure resource allocation scheme and confirm the theoretical analysis.

Acknowledgements This work was supported in part by National Mobile Communications Research Laboratory, Southeast University (Grant No. 2023D03), National Key R&D Program of China (Grant No. 2023YFB2904804), and National Natural Science Foundation of China (Grant Nos. 62394292, 62394290).

Supporting information Appendixes A–D. The supporting information is available online at info.scichina.com and link.springer.com. The supporting materials are published as submitted, without typesetting or editing. The responsibility for scientific accuracy and content remains entirely with the authors.

References

1 Zhao Z, Yang Z, Huang C, et al. A joint communication and computation design for distributed RIS-assisted probabilistic semantic communication in IIoT. IEEE Int Things J, 2024, 11: 26568–26579
2 Yang W, Du H, Liew Z Q, et al. Semantic communications for future Internet: fundamentals, applications, and challenges. IEEE Commun Surv Tut, 2023, 25: 213–250
3 Xu W, Yang Z, Ng D W K, et al. Edge learning for B5G networks with distributed signal processing: semantic communication, edge computing, and wireless sensing. IEEE J Sel Top Signal Process, 2023, 17: 9–39
4 Dai J, Li L, Yang Z, et al. Sum rate maximization for probalistic semantic communication via compression ratio optimization. IEEE Commun Lett, 2024, 28: 2829–2833
5 Xue J, Ratnarajah T, Zhong C, et al. Reliability analysis for large MIMO systems. IEEE Wireless Commun Lett, 2022, 3: 553–556
6 Du H, Wang J, Niyato D, et al. AI-generated incentive mechanism and full-duplex semantic communications for information sharing. IEEE J Sel Areas Commun, 2023, 41: 2981–2997
7 Farsad N, Rao M, Goldsmith A. Deep learning for joint source-channel coding of text. In: Proceedings of IEEE International Conference on Acoustics, Speech and Signal Processing (ICASSP), Calgary, 2018. 2326–2330
8 Xie H, Qin Z, Li G Y, et al. Deep learning enabled semantic communication systems. IEEE Trans Signal Process, 2021, 69: 2663–2675
9 Xu J, Ai B, Chen W, et al. Wireless image transmission using deep source channel coding with attention modules. IEEE Trans Circ Syst Video Technol, 2022, 32: 2315–2328
10 Tong H, Yang Z, Wang S, et al. Federated learning based audio semantic communication over wireless networks. In: Proceedings of IEEE Global Communications Conference (GLOBECOM), Madrid, 2021. 1–6
11 Yang Z, Chen M, Liu Y, et al. A joint communication and computation framework for digital twin over wireless networks. IEEE J Sel Top Signal Process, 2024, 18: 6–17

12 Yang Z, Chen M, Zhang Z, et al. Energy efficient semantic communication over wireless networks with rate splitting. IEEE J Sel Areas Commun, 2023, 41: 1484–1495
13 Su J, Liu Z, Xie Y, et al. Semantic communication-based dynamic resource allocation in D2D vehicular networks. IEEE Trans Veh Technol, 2023, 72: 10784–10796
14 Zhang H, Wang H, Li Y, et al. Toward intelligent resource allocation on task-oriented semantic communication. IEEE Wireless Commun, 2023, 30: 70–77
15 Yu Y, Liu S, Yuan W, et al. Robust secure beamforming for multi-receiver multi-eavesdropper MIMO SWIPT systems. In: Proceedings of IEEE Global Communications Conference, Taipei, 2020. 1–6
16 Yang Z, Xu W, Liang L, et al. On privacy, security, and trustworthiness in distributed wireless large AI models (WLAM). 2024. ArXiv:2412.02538
17 Lv L, Xu D, Hu R Q, et al. Safeguarding next-generation multiple access using physical layer security techniques: a tutorial. Proc IEEE, 2024, 112: 1421–1466
18 Lv L, Wu Q, Li Z, et al. Covert communication in intelligent reflecting surface-assisted NOMA systems: design, analysis, and optimization. IEEE Trans Wireless Commun, 2022, 21: 1735–1750
19 Deng Z, Gao Y, Cai C. Joint resource allocation for secrecy wireless powered communication networks with an active eavesdropper. In: Proceedings of the 3rd IEEE International Conference on Computer and Communications (ICCC), Chengdu, 2017. 633–636
20 Pirayesh H, Zeng H. Jamming attacks and anti-jamming strategies in wireless networks: a comprehensive survey. IEEE Commun Surv Tut, 2022, 24: 767–809
21 Tung T Y, Gündüz D. Deep joint source-channel and encryption coding: secure semantic communications. In: Proceedings of IEEE International Conference on Communications, Rome, 2023. 5620–5625
22 Yang Y, Shikh-Bahaei M, Yang Z, et al. Secure design for integrated sensing and semantic communication system. In: Proceedings of IEEE Wireless Communications and Networking Conference (WCNC), Dubai, 2024. 1–7
23 Payaro M, Pascual-Iserte A, Lagunas M. Robust power allocation designs for multiuser and multiantenna downlink communication systems through convex optimization. IEEE J Sel Areas Commun, 2007, 25: 1390–1401
24 Yu X, Xu D, Sun Y, et al. Robust and secure wireless communications via intelligent reflecting surfaces. IEEE J Sel Areas Commun, 2020, 38: 2637–2652
25 Vu Q D, Tran L N, Juntti M. On spectral efficiency for multiuser MISO systems under imperfect channel information. IEEE Trans Veh Technol, 2021, 70: 1946–1951
26 Pascual-Iserte A, Palomar D P, Perez-Neira A I, et al. A robust maximin approach for MIMO communications with imperfect channel state information based on convex optimization. IEEE Trans Signal Process, 2006, 54: 346–360
27 Zhang J F, Lu W D, Xing C W, et al. Intelligent integrated sensing and communication: a survey. Sci China Inf Sci, 2025, 68: 131301
28 Xiao Y, Wang E H, Chen Y F, et al. Communication-centric integrated sensing and communications with mixed fields. Sci China Inf Sci, 2024, 67: 219301
29 Cheng X, Duan D, Gao S, et al. Integrated sensing and communications (ISAC) for vehicular communication networks (VCN). IEEE Internet Things J, 2022, 9: 23441–23451
30 Han C, Zhang G, Ji B, et al. On the potential of using emerging microwave links for city rainfall monitoring. IEEE Commun Mag, 2023, 61: 174–180
31 Zhu G X, Lyu Z H, Jiao X, et al. Pushing AI to wireless network edge: an overview on integrated sensing, communication, and computation towards 6G. Sci China Inf Sci, 2023, 66: 130301
32 Du H, Wang J, Niyato D, et al. Semantic communications for wireless sensing: RIS-aided encoding and self-supervised decoding. IEEE J Sel Areas Commun, 2023, 41: 2547–2562
33 Wang S H, Hong Y W P. Transmission control with imperfect CSI in channel-aware slotted ALOHA networks. IEEE Trans Wireless Commun, 2023, 8: 5214–5224
34 Xiong Y, Liu F, Cui Y, et al. On the fundamental tradeoff of integrated sensing and communications under gaussian channels. IEEE Trans Inform Theor, 2023, 69: 5723–5751
35 Yan L, Qin Z, Zhang R, et al. Resource allocation for text semantic communications. IEEE Wireless Commun Lett, 2022, 11: 1394–1398
36 Dong C, Liang H, Xu X, et al. Semantic communication system based on semantic slice models propagation. IEEE J Sel Areas Commun, 2023, 41: 202–213
37 Chen P, Ouyang J, Zhu W P, et al. Artificial-noise-aided energy-efficient secure beamforming for multi-eavesdroppers in cognitive radio networks. IEEE Syst J, 2020, 14: 3801–3812
38 Hong S, Pan C, Ren H, et al. Robust transmission design for intelligent reflecting surface-aided secure communication systems with imperfect cascaded CSI. IEEE Trans Wireless Commun, 2021, 20: 2487–2501